Supplemental Material: Impact of Many-Body Effects on Landau Levels in Graphene

J. Sonntag,[1,2] S. Reichardt,[1,3] L. Wirtz,[3] B. Beschoten,[1]

M. I. Katsnelson,[4] F. Libisch,[5] and C. Stampfer[1,2]

[1]*JARA-FIT and II. Institute of Physics,*

RWTH Aachen, 52074 Aachen, Germany

[2]*Peter Grünberg Institute (PGI-9), Forschungszentrum Jülich, 52425 Jülich, Germany*

[3]*Physics and Materials Science Research Unit,*

University of Luxembourg, L-1511 Luxembourg, Luxembourg

[4]*Radboud University, Institute for Molecules and Materials, 6525AJ Nijmegen, Netherlands*

[5]*Institute for Theoretical Physics, Vienna University of Technology, 1040 Vienna, Austria*

(Dated: November 29, 2017)

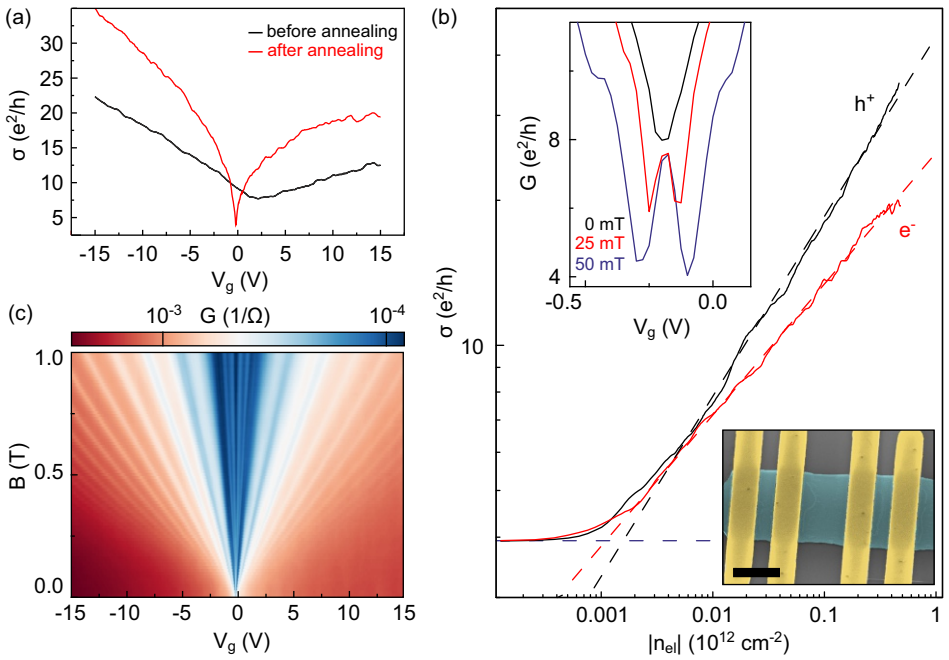

FIG. S1. (a) Electrical conductivity σ as a function of gate voltage V_g of the suspended graphene sample before and after current annealing. Measurements are taken at $T = 4.2$ K. (b) Double logarithmic graph of the conductivity σ after current annealing as a function of charge carrier density for holes (black) and electrons (red). The red and black dashed lines are linear fits outside the regime of charge inhomogeneity. The purple, horizontal, dashed line indicates the minimum conductivity due to charge inhomogeneity. The crossing point of these lines defines n^*. The left inset shows the onset of SdHO at approx. 25 mT, indicating a mobility $\mu \approx 400\,000\,\mathrm{cm}^2/(\mathrm{Vs})$. The right inset depicts a false-color scanning electron micrograph of the measured device. The scale bar represents 2 µm. (c) Electrical conductivity as a function of magnetic field and gate voltage, used to determine back gate the lever-arm $\alpha = 3.15 \times 10^{10}\,\mathrm{cm}^{-2}\mathrm{V}^{-1}$.

THEORY OF MAGNETO-PHONON RESONANCES IN SINGLE-LAYER GRAPHENE

Following Ando [1], Goerbig *et al.* [2], and Neumann *et al.* [3], we calculate the Raman G mode phonon frequency ω_G and line width Γ_G as the real and doubled negative imaginary part, respectively, of the root of the following equation:

$$\omega^2 - (\omega_0 - i\gamma_0/2)^2 = 2(\omega_0 - i\gamma_0/2)\Pi(\omega), \tag{S1}$$

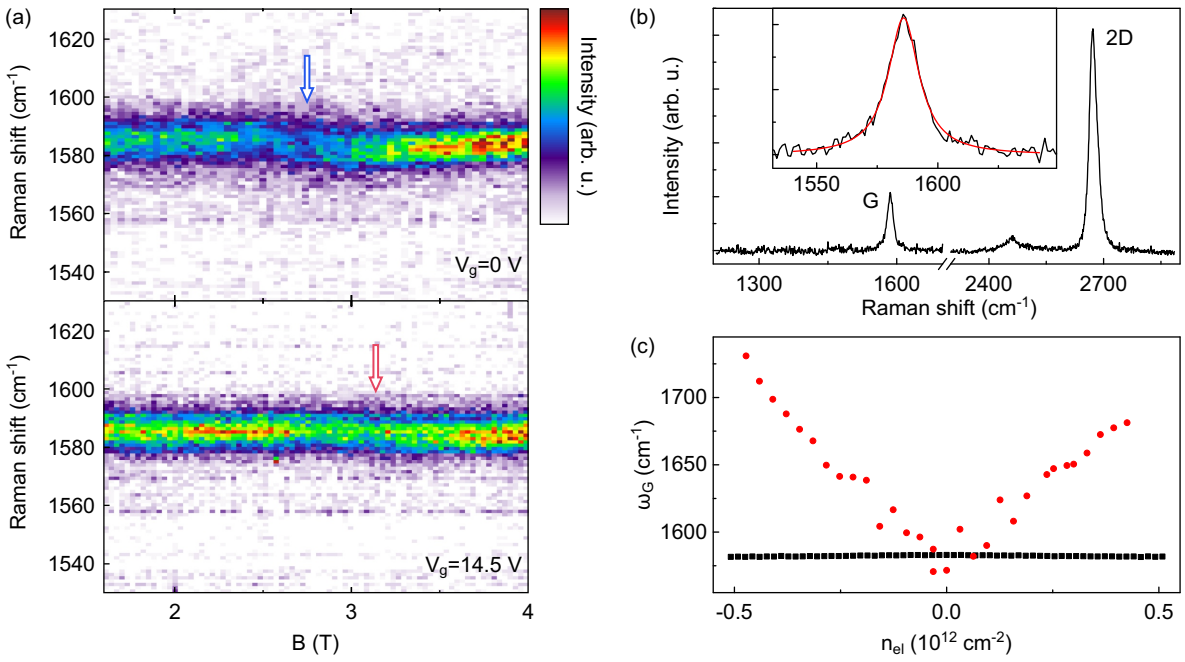

FIG. S2. (a) Raman intensity around the G peak plotted as a function of the magnetic field around the T_1-MPR at $V_g = 0\,\mathrm{V}$ and $V_g = 14.5\,\mathrm{V}$. The arrows indicate the positions of the T_1-MPRs as extracted in the main text. (b) Raman spectrum taken at $V_g = 0\,\mathrm{V}$ and $B = 0\,\mathrm{T}$. the inset depicts a Lorentzian fit of the G peak. (c) Illustration of the change in ω_G required to observe the shift in B_{T_1} as seen in Fig. 2 in the main text under the assumption of a constant $v_F = 1.06 \times 10^6$ m/s (red dots). Black squares represent the actually measured ω_G as a function of charge carrier density at zero magentic field.

where the phonon self-energy $\Pi(\omega)$ is given by

$$\Pi(\omega) = e v_F^2 B \lambda \sum_{n=0}^{\infty} \left[\frac{\left(\bar{\nu}_{-n} - \bar{\nu}_{n+1} - \bar{\nu}_n + \bar{\nu}_{-(n+1)}\right)(T_n - i\gamma_{el}/2)}{\omega^2 - (T_n - i\gamma_{el}/2)^2} + \frac{2}{T_n - i\gamma_{el}/2} \right]. \qquad \text{(S2)}$$

Here, $T_n = \frac{1}{\hbar}|\varepsilon_{n+1} + \varepsilon_n|$ are the frequencies associated with the inter-Landau level transitions, and $\varepsilon_{\pm n} = \pm v_{F,n}\sqrt{2e\hbar Bn}$ is the energy of the $\pm n$th Landau level as stated in the main text. $\bar{\nu}_n = (\nu - 4n + 2)/4$ denotes the partial filling factor, which depends on the filling factor $\nu = n_{el}h/(eB)$ and obeys $0 \leq \bar{\nu}_n \leq 1$. γ_{el} introduces a damping of the Landau level excitations to account for their finite lifetimes and γ_0 represents the damping of the phonon mode due to anharmonic effects. The dimensionless electron-phonon coupling constant is denoted by λ. By fitting the root of Eq. S1 to all our MPR measurements we get a set of average parameters leading to: $\omega_0 = 1584.8\,\mathrm{cm}^{-1}$, $\gamma_0 = 7.6\,\mathrm{cm}^{-1}$, $\gamma_{el} = 395\,\mathrm{cm}^{-1}$,

$\lambda = 4 \times 10^{-3}$ and $v_\mathrm{F} = 1.33 \times 10^6\,\mathrm{m/s}$, which we then use to calculate the maximum width $\Gamma^{\max}_{\mathrm{G},T_1}$ at the resonance B_{T_1} as a function of charge carrier density, as represented by the blue line in Fig. 2a in the main text.

TIGHT-BINDING MODEL

We use a third-nearest neighbor tight-binding description of graphene [4] to evaluate the Coulomb and exchange contributions required for the self-energy correction $\Sigma^{\mathrm{HF}}_{\pm n}$. We include the magnetic field via a Peierls phase factor and eliminate edge states by a finite mass boundary term at the zigzag edges [4]. We use an Arnoldy-Lanczos algorithm in conjunction with shift-invert [5] to calculate approximately 3000 eigenstates (in groups of 400 for efficiency) of a quadratic graphene flake of size 40×40 nm^2 at a magnetic field of 200 T. The Coulomb and exchange contributions are evaluated as

$$v^{\mathrm{Hart.}}_{i,j} = e^2 \langle ij| \frac{1}{|\vec{r}_1 - \vec{r}_2|} |ij\rangle \tag{S3}$$

and

$$v^{\mathrm{Fock}}_{i,j} = e^2 \langle ji| \frac{1}{|\vec{r}_1 - \vec{r}_2|} |ij\rangle \,. \tag{S4}$$

Considering the scaling invariance of the Dirac equation, we rescale our results down to the experimental field strength ($l_B \propto 1/\sqrt{B}$). Effectively, our results thus correspond to an $\approx 330 \times 330$ nm^2-sized flake. We evaluate both contributions for all pairs of eigenstates. The state indices i and j can each be split into a Landau level index $\pm n$ and a quantum number m, that labels the degenerate states, as described in the main manuscript, i.e., $i = (\pm n, m)$, $j = (\pm n', m')$. Eigenstates are assigned to specific Landau levels $\pm n$ and $\pm n'$ based on their energy. Due to the finite size of our system, there are a few states within the energy gaps between the Landau levels, which we do not include in the evaluation of the self energy.

TEMPERATURE-DEPENDENT SHUBNIKOV-DE-HAAS OSCILLATIONS

To extract the renormalization of v_F at low magnetic fields, we closely follow the method used by Elias *et al.* [6] and perform temperature-dependent Shubnikov-de Haas oscillation measurements. We measure the conductivity σ as a function of charge carrier density for different temperatures in a range of $T = 4$ K to $T = 60$ K at a magnetic field of $B = 0.25$ T

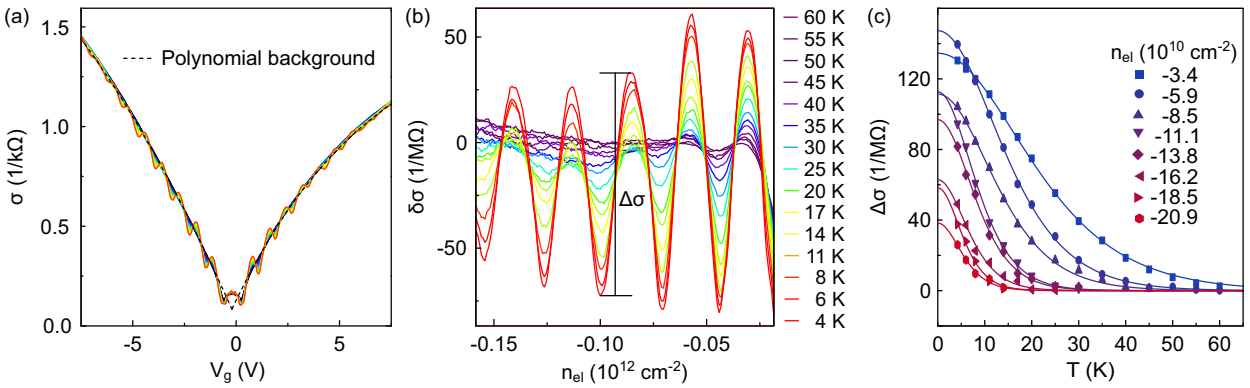

FIG. S3. (a) Electrical conductivity as a function of applied gate voltage V_g for different temperatures at a magnetic field of $B = 0.25$ T. The dashed line represent a fit of a polynomial background for both electron and hole doping. (b) Shubnikov-de Haas oscillations at $B = 0.25$ T after subtraction of a polynomial background. (c) Height of the oscillations $\Delta\sigma$ as a function of temperature for different charge carrier densities.

(see Fig. S3a). For electrons and holes we separately fit a 4th-order polynomial to the smooth, high temperature data and subtract this background from all measurements. The resulting conductivity oscillations $\delta\sigma$ are shown exemplary in Fig. S3b for the hole side. We extract the amplitude of the Shubnikov-de Haas oscillations as the difference $\Delta\sigma$ between maxima and minima (see label in Fig. S3b). This makes the extracted amplitude almost independent of the chosen background. The amplitude as a function of temperature (T) for different hole densities are presented in Fig. S3c. The amplitude follow the Lifshitz-Kosevich formula [7]:

$$\Delta\sigma \propto T/\sinh\left(2\pi^2 k_\mathrm{B} T \frac{m_\mathrm{c}}{e\hbar B}\right), \tag{S5}$$

where $m_c = \hbar\sqrt{\pi n_\mathrm{el}}/v_\mathrm{F}$ is the cyclotron mass at a given n_el. By fitting this expression to our data (see Fig. S3c), we are able to extract v_F for different charge carrier densities, which is shown in the inset in Fig. 3 in the main text.

FINITE RENORMALIZATION OF THE FERMI VELOCITY IN PRESENCE OF LANDAU LEVELS

As shown by González *et al.* [8], for two-dimensional massless Dirac fermions interacting via the Coulomb potential, the Fock contribution to the Fermi velocity is logarithmically

divergent in the limit of zero temperature and chemical potential. The corresponding Fock contribution to the Hamiltonian is:

$$\hat{H}_F = \sum_{\vec{k}} \sum_{\alpha,\beta} \hat{\Psi}^{\dagger}_{\alpha}(\vec{k}) h_{\alpha\beta}(\vec{k}) \hat{\Psi}_{\beta}(\vec{k}), \tag{S6}$$

where $\hat{\Psi}_{\beta}(\vec{k})$ is the annihilation operator for the Dirac fermion with the quasi-wave vector $\vec{k}$ and pseudospin projection β,

$$h_{\alpha\beta}(\vec{k}) = -2\pi e^2 \sum_{\vec{k'}} \frac{\rho_{\beta\alpha}(\vec{k'})}{|\vec{k} - \vec{k'}|}, \tag{S7}$$

and $\rho_{\beta\alpha}(\vec{k}) = \langle \hat{\Psi}^{\dagger}_{\vec{k}\alpha} \hat{\Psi}_{\vec{k}\beta} \rangle$ is the single-particle density matrix ([9], Sect. 8.4). Its spinor structure is given by the expression:

$$\hat{\rho}_{\vec{k}} = n_{\vec{k}} \hat{I} + \vec{m}_{\vec{k}} \hat{\vec{\sigma}}, \tag{S8}$$

where $\hat{I}$ is the 2×2 unit matrix, $\hat{\vec{\sigma}}$ are the Pauli matrices and the pseudospin density $\vec{m}_{\vec{k}}$ has the form $\vec{m}_{\vec{k}} = \vec{k} F(k)$. Following Ref. [9], Sect. 7.2, for chemical potential and temperature equal to zero

$$F(k) = \frac{1}{2k}. \tag{S9}$$

Then the Fock contribution to the Fermi velocity reads ([9], Sect. 8.4):

$$\delta v_{\mathrm{F}} = \frac{\pi e^2}{\hbar} \sum_{\vec{k}} \frac{F(k)}{k} = \frac{e^2}{2\hbar} \int_0^{\Lambda} \mathrm{d}k \, F(k), \tag{S10}$$

where $\Lambda \propto 1/a$ is the ultraviolet (UV) cutoff due to the inapplicability of the Dirac model at large wave vectors and a is the interatomic distance of the graphene lattice. Explicit numerical calculations on a lattice for the case of a pure Coulomb interaction [10] give the value $\Lambda \approx 0.8/a$. When substituting Eq. S9 into Eq. S10 we have a divergence at the lower limit, which, at finite charge carrier density, is cut off at the Fermi wave vector k_{F}. The result reads:

$$\delta v_{\mathrm{F}} = \frac{e^2}{4\hbar} \ln\left(\frac{\Lambda}{k_{\mathrm{F}}}\right). \tag{S11}$$

In the presence of a magnetic field, the density matrix Eq. S8 and therefore the function $F(k)$ can be calculated using the explicit expression for the Green's function of massless Dirac electrons in the presence of a magnetic field found in Ref. [11]. The result is

$$F(k) = \frac{l_B}{2\sqrt{\pi}} \int_0^{\infty} \mathrm{d}s \, \frac{\exp(-k^2 l_B^2 \tanh(s))}{\sqrt{s} \cosh(s)^2}, \tag{S12}$$

where $l_B = \sqrt{\hbar/(eB)}$ is the magnetic length. Substituting Eq. S12 into Eq. S10 and changing the order of integrations we obtain

$$\delta v_{\rm F} = \frac{e^2}{8\hbar}\int_0^\infty {\rm d}s\, \frac{{\rm erf}(\Lambda l_B\sqrt{\tanh(s)})}{\sqrt{s\tanh(s)}\cosh(s)^2}, \tag{S13}$$

where

$${\rm erf}(x) = \frac{2}{\sqrt{\pi}}\int_0^x {\rm d}s\, \exp(-x^2) \tag{S14}$$

is the error function. Assuming that $\Lambda l_B \gg 1$, one can calculate the integral in Eq. S13 by splitting the integration interval into two parts: $(0,\infty) = (0,C) + (C,\infty)$ with some $1/(\Lambda l_B)^2 \ll C \ll 1$. With logarithmic accuracy, one has, instead of Eq. S11,

$$\delta v_{\rm F} = \frac{e^2}{4\hbar}\ln(\Lambda l_B). \tag{S15}$$

Thus the infrared divergence (Eq. S11) is cut off at wave vectors on the order of the inverse magnetic length and the dependence of the Fermi velocity on the electron filling factor is no longer singular in the presence of a magnetic field.

[1] T. Ando, J. Phys. Soc. Jpn. **76**, 024712 (2007).

[2] M. O. Goerbig, J.-N. Fuchs, K. Kechedzhi, and V. I. Fal'ko, Phys. Rev. Lett. **99**, 087402 (2007).

[3] C. Neumann, S. Reichardt, M. Drögeler, B. Terrés, K. Watanabe, T. Taniguchi, B. Beschoten, S. V. Rotkin, and C. Stampfer, Nano Lett. **15**, 1547 (2015).

[4] L. Chizhova, J. Burgdörfer, and F. Libisch, Phys. Rev. B **92**, 125411 (2015).

[5] C. Lanczos, *An iteration method for the solution of the eigenvalue problem of linear differential and integral operators* (United States Governm. Press Office Los Angeles, CA, 1950).

[6] D. Elias, R. Gorbachev, A. Mayorov, S. Morozov, A. Zhukov, P. Blake, L. P. I. Grigorieva, K. Novoselov, F. Guinea, and A. Geim, Nat. Phys. **7**, 701 (2011).

[7] S. Sharapov, V. Gusynin, and H. Beck, Phys. Rev. B **69**, 075104 (2004).

[8] J. González, F. Guinea, and M. Vozmediano, Nucl. Phys. B **424**, 595 (1994).

[9] M. Katsnelson, *Graphene: Carbon in Two Dimensions* (Cambridge University Press, 2012).

[10] N. Y. Astrakhantsev, V. V. Braguta, and M. I. Katsnelson, Phys. Rev. B **92**, 245105 (2015).

[11] V. Gusynin, V. Miransky, and I. Shovkovy, Physical Review D **52**, 4718 (1995).